frontiers | Frontiers in Built Environment

TYPE Original Research
PUBLISHED 08 October 2025
DOI 10.3389/fbuil.2025.1643931

OPEN ACCESS

EDITED BY
Saubhagya Kumar Panigrahi,
Veer Surendra Sai University of Technology, India

REVIEWED BY
Mohammad M. Karimi,
Tarbiat Modares University, Iran
Qinwen Tan,
China University of Geosciences Wuhan, China

*CORRESPONDENCE
Wenhua Zheng,
1443285026@qq.com

RECEIVED 09 June 2025
ACCEPTED 18 September 2025
PUBLISHED 08 October 2025

CITATION
Zheng C, Li W, Liu C, Zheng W, Cheng W, You P and Li X (2025) Mechanical simulation and engineering utilization of limestone tailings in roadbed construction. *Front. Built Environ.* 11:1643931. doi: 10.3389/fbuil.2025.1643931

Mechanical simulation and engineering utilization of limestone tailings in roadbed construction

Chunyu Zheng[1], Wenwei Li[1], Chenxu Liu[2], Wenhua Zheng[2]*, Wei Cheng[1], Pengchao You[2] and Xingjia Li[2]

[1]No.1 Engineering Co., Ltd., CCCC First Highway Engineering, Beijing, China, [2]School of Civil and Transportation Engineering, Beijing University of Civil Engineering and Architecture, Beijing, China

This study investigates the engineering utilization of limestone tailings as subgrade filling material through comprehensive material characterization and mechanical simulation. Material properties were analyzed using laser particle size detection, XRD, and SEM, while mechanical behavior was assessed via direct shear and triaxial shear tests, revealing cohesion and internal friction angle values of 1.97 kPa and 30.67°, respectively, both complying with subgrade technical specifications. Integrating the case of the G207 Xiangyang reconstruction project, ABAQUS-based finite element simulations of conventional replacement scenarios showed a maximum settlement of 1.743×10^{-1} m at 5 m replacement depth under 25 kPa loading, which deviated by only 5.6% from field measurements and fully met highway standards. The validated computational framework establishes limestone tailings as a viable and sustainable alternative to natural soil, reducing resource consumption while maintaining structural integrity.

KEYWORDS

limestone tailings, subgrade fillers, shearing strength, numerical simulation, subgrade settlement

1 Introduction

Tailings are one of the largest solid waste materials in China, with the total stockpile reaching 23.1 billion tons by 2020 (Yu and Du, 2023; Su et al., 2024). Currently, most tailings are still disposed of in tailing ponds, leading to environmental pollution and posing significant safety risks (Liu H. B. et al., 2024; Adewuyi et al., 2024; Maruthupandian et al., 2021; Singh et al., 2024). Among these, cement tailings, a byproduct of cement production, also known as limestone tailings, represent a considerable volume of non-metallic tailings. The primary components of limestone tailings are calcite and quartz. During cement production, specific requirements are set for the chemical composition of limestone (Song et al., 2021). However, due to significant variations in the CaO and MgO content across different limestone sources, many types of limestone are unsuitable for cement production, resulting in the generation of a large volume of limestone tailings (Zhang M et al., 2025). Although limestone tailings cannot be used in cement production, they still possess certain aggregate properties, making them viable for use as engineering materials

(Li et al., 2025; Xu et al., 2025; Gallage et al., 2024). This is an effective way for high-value utilization of tailings materials (Wang Y. S et al., 2022; Gou et al., 2019; Zhou et al., 2021; Wang Z. Q et al., 2022).

China has a complex and diverse geological landscape, and soft soils are widely distributed across many regions (Liu et al., 2022). In these soft soil regions, highway construction often encounters significant geotechnical challenges, such as excessive total settlement, differential settlement, and long-term post-construction deformation, primarily due to the low bearing capacity and high compressibility of soft soils, coupled with traffic loads and the self-weight of embankments (Xu et al., 2019; Sun et al., 2021; Liao et al., 2025; Gupta et al., 2025). These issues can lead to pavement cracking, structural instability, and increased maintenance costs, thereby threatening the safety and durability of highways. Therefore, accurately understanding the settlement characteristics of soft soil subgrades and adopting effective and appropriate settlement control methods have become urgent issues that need to be addressed in highway construction in soft soil regions (Xiong et al., 2022). In this case, it is a promising option to directly use the base-treated tailings material as a highway engineering material (Gao et al., 2025; Liu Hongbo et al., 2024; Wu et al., 2024). Utilizing them not only helps address the settlement challenges of soft soils but also aligns with the requirements of the Highway Subgrade Construction Technical Specifications (JTG/T 3610–2019). Furthermore, this approach promotes the recycling and resource utilization of industrial solid waste, thereby achieving dual benefits in engineering economy and environmental sustainability (Panchal et al., 2018; Liang et al., 2024; Ou et al., 2022; Chu et al., 2023) mixed iron tailings and carbide slag, and physically and chemically modified them to inhibit water sensitivity, as a sub-level backfill material for engineering practice. The results show that the free expansion index of expansive soil modified by solid waste such as iron tailings is reduced to less than 30%, which meets the requirements of expressway subgrade (Kong et al., 2024). Prepared road subbase specimens with a high proportion of fine iron tailing. The road subbase specimen achieved a 7-day unconfined compressive strength of 1.97 MPa and an elastic modulus of 286 MPa, demonstrating good mechanical properties. This technology provides a paradigm for the comprehensive utilization of fine iron tailings and the preparation of new road subbase materials (Yin et al., 2024). Investigated pure nickel–iron slag mechanical properties and road performance as a roadbed fill material. the results show that the particle size distribution of pure nickel-iron slag is not good, mainly lacking particles in the range of 0.075–0.25 mm. Adding 30%–40% clay can effectively improve the particle size distribution of ferronickel slag. After modification by adding clay, the particle size distribution of the modified ferronickel slag soil is good, which meets the requirements of roadbed design (Zhu et al., 2024). Studied investigates the efficacious utilization of sludge as a subgrade filler through *in-situ* shallow stabilization, employing cementitious industrial waste materials, including steel slag, fly ash, and calcium carbide residue, as binding agents (Zhao et al., 2024). Used the phosphate tailings employed to modify clay, forming a phosphate tailings-modified clay applied in the subgrade to improve the utilization rate of phosphate tailings and widen the sources of subgrade filler. The analysis demonstrates that the better strength mainly comes from the skeleton role of phosphate tailings and the cementation of clay. The systematic laboratory test results and economic analysis collectively provide data evidence for the advantages of phosphate tailings-modified clay as a subgrade filler. Shanmugasundaram evaluated the magnesite mine tailings application as subgrade in road construction, X-ray Diffraction (XRD), Field emission Scanning Electron Microscope (SEM), and Energy-Dispersive X-ray spectroscopy (EDX) analyses were carried out to explore the stabilization mechanisms, this study finds that the cement treated magnesite mine tailings can be used as a subgrade in road construction which will not only reduce the negative environmental effects of open dumping of magnesite mine tailings but also replaces the natural soil in subgrade construction (Shanmugasundaram and Shanmugam, 2023; Zhang Z. Q et al., 2025) presents a novel approach to upcycling low-grade shield spoil tailings (SST, containing 19.41% kaolinite and 29.88% illite) as supplementary cementitious materials, addressing both waste valorization and carbon reduction challenges (de Matos et al., 2025). Prepared limestone calcined clay cement using calcined kaolinite iron ore tailings and ceramic tile waste instead of natural calcined clay (Sa et al., 2022). Evaluated soil-cement mixtures with different proportions of soil and iron ore tailings, the results show that the addition of 10% and 20% of iron ore tailings showed a decline in the compression resistance, but all the mixtures met the required strength standard for a base layer application, the used of iron ore tailings in pavements layers also contributes by creating a new disposal method to the tailings, reducing the environmental impact related to the mining activity, and it possibly can reduce the costs related to the pavement construction.

This paper aims to evaluate the feasibility of utilizing limestone tailings as subgrade fill material, thereby promoting the sustainable reuse of industrial solid waste. To achieve this, the study first characterizes the physical and chemical properties of limestone tailings based on their intrinsic material attributes. Subsequently, their mechanical behavior is investigated through laboratory experiments, including compaction and direct shear tests. In addition, numerical simulations are carried out to analyze the performance of embankments constructed with limestone tailings, particularly focusing on the prediction of maximum settlement under varying vehicle loads and fill depths. Finally, the experimental and simulation results are compared with relevant engineering standards to comprehensively assess the suitability of limestone tailings for subgrade applications. The findings of this study are expected to provide technical support for the resource utilization of limestone tailings, contributing to environmental protection and sustainable infrastructure development.

2 Materials

2.1 Limestone tailings

The limestone tailings used in the experiments were sourced from the tailings pond of Xiangyang Huaxin Cement Co., Ltd. The physical parameters are presented in Table 1. Additionally, the chemical composition of the limestone tailings was determined through X-ray photoelectron spectroscopy (XPS) and XRD analysis, with the detailed results shown in Table 2 and Figure 1.

As shown in Table 2, the primary chemical components of the limestone tailings are CaO, SiO_2, and Al_2O_3, with CaO and SiO_2

10.3389/fbuil.2025.1643931

TABLE 1 Physical parameters of limestone tailings.

Materials	Physical parameters				
	Liquid limit/%	Plastic limit/%	Moisture content/%	Loss on ignition/%	Plasticity index
Limestone tailings	29.1	17.7	2	0.25	11.4

TABLE 2 Chemical composition of limestone tailings.

Materials	Chemical composition/%								
	CaO	SiO_2	Al_2O_3	Fe_2O_3	MgO	K_2O	TiO_2	SO_3	Na_2O
Limestone tailings	65.99	18.71	7.57	3.24	1.73	1.34	0.79	0.16	0.47

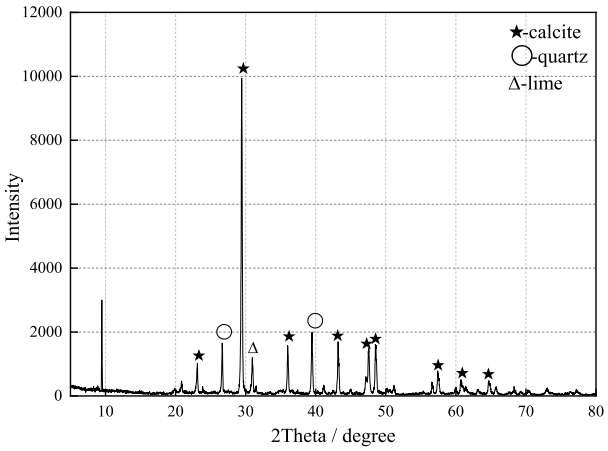

FIGURE 1
XRD analysis of limestone tailings.

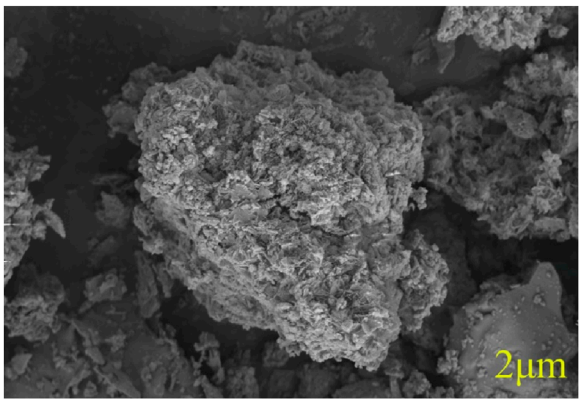

FIGURE 2
SEM images of the limestone tailings.

accounting for over 80% of the material's composition. Figure 1 reveals that the main mineral components of the limestone tailings are quartz and calcite. The microstructure of limestone tailings was observed using a scanning electron microscope (ZEISS Gemini SEM 300, Germany), as shown in Figure 2. The SEM images show that the particles possess angular and irregular shapes, which enhance inter-particle friction and mechanical interlocking. This geometry restricts particle rotation and sliding under stress, thereby increasing shear resistance. Furthermore, XRD analysis indicates that calcite and quartz are the dominant mineral phases. These minerals are characterized by hardness and surface roughness, which improve contact friction between particles. Despite the relatively low cohesion resulting from limited cementation, the combination of angular morphology and mineral composition leads to a notably high internal friction angle. This mechanistic link between microstructure and macroscopic strength highlights the suitability of limestone tailings as a subgrade fill material.

The limestone tailings used in this study were obtained from the tailings pond of Xiangyang Huaxin Cement Co., Ltd. Before testing, the material underwent basic pretreatment to ensure consistency. Large debris and visible impurities were manually removed, and the tailings were air-dried to achieve a stable moisture state before specimen preparation. Representative samples were sieved in accordance with JTG 3430-2020 to determine the particle size distribution, as presented in Figure 3. No additional grinding or chemical treatment was carried out; therefore, the gradation shown reflects the intrinsic particle characteristics of the tailings after minimal physical conditioning. It should be noted that such pretreatment mainly stabilizes moisture content and eliminates oversized particles, which helps reduce variability in compaction and strength tests. Similar to gravel gradation, the limestone tailings have particle sizes concentrated in the range of 0–19 mm, with the majority of the limestone tailings particles falling within the 1.18–9.5 mm range, accounting for approximately 70% of the total particle size distribution. The corresponding d60, d30, and d10 values are 4 mm, 0.9 mm, and 0.13 mm, respectively. The uniformity coefficient, calculated as Cu = 31.2 (>5), indicates that the limestone tailings have good gradation, with a continuous particle size distribution and no gaps. The fine particles can effectively fill the voids between the coarser particles, demonstrating a certain degree of filling effect (Zhang et al., 2024).

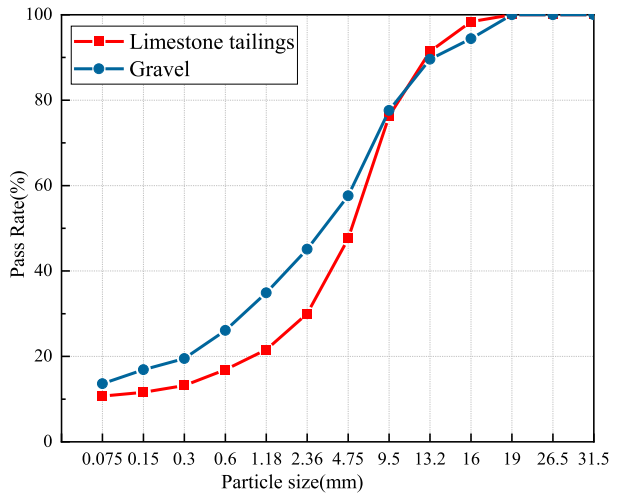

FIGURE 3
Gradation curve of limestone tailings and gravel.

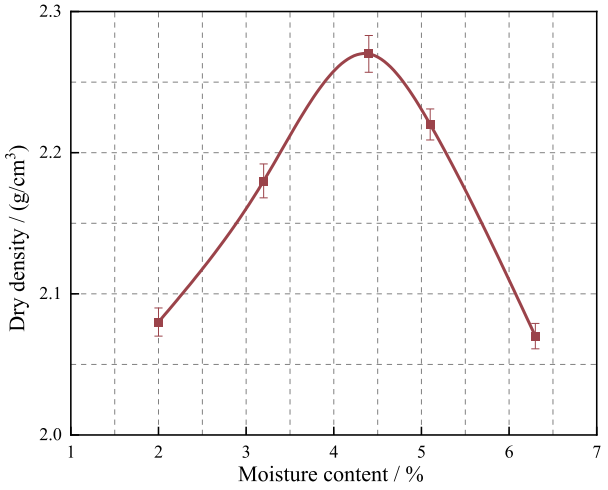

FIGURE 4
Dry density and moisture content curve of limestone tailings.

3 Test methods and results

3.1 Compaction test

According to the Highway Geotechnical Testing Procedures (JTG 3430-2020), standard Proctor compaction tests were conducted on limestone tailings to determine their compaction characteristics. Five different moisture contents (2%, 3%, 4%, 5%, and 6%) were selected to capture the typical range of water content in field applications and to identify the optimum moisture content for compaction accurately. For each moisture content group, three parallel test specimens were prepared and tested to ensure data reliability and repeatability. The average values of the test results are presented in Figure 4. The compaction curve derived from the test data shows a clear peak, indicating a well-defined compaction behavior. The results reveal that the limestone tailings exhibit an optimum moisture content of 4.3%, corresponding to a maximum dry density of 2.283 g/cm^3. This suggests that under appropriate moisture conditions, limestone tailings can achieve a relatively high degree of compaction, making them potentially suitable for use as subgrade fill material.

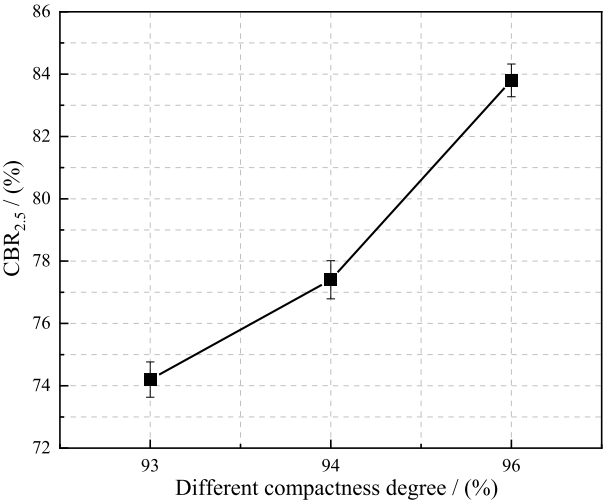

FIGURE 5
The CBR of limestone tailings under different compactness.

3.2 California bearing ratio test (CBR)

To evaluate the load-bearing performance of limestone tailings under different compaction conditions, three groups of samples were prepared with compaction densities of 93%, 94%, and 96%, respectively. Each group consisted of three parallel specimens to ensure data consistency and reliability. The CBR tests were carried out by the procedures outlined in JTG 3430–2020, and the results are presented in Figure 5. As shown in Figure 5, the CBR values increase with compaction density, indicating that higher compaction improves the material's load-bearing capacity. Notably, even at the lowest compaction density of 93%, the CBR at 2.5 mm penetration ($CBR_{2.5}$) reached 74.2%, which is substantially higher than the minimum required value of 8% specified in the Technical Specifications for Construction of Highway Subgrades (JTG/T 3610–2019) for subgrade replacement materials. This demonstrates that the limestone tailings possess excellent load-bearing characteristics, even under relatively low compaction levels. The results confirm the suitability of limestone tailings as a substitute for conventional subgrade fill, particularly in soft soil areas where subgrade replacement is needed to improve foundation stability. Furthermore, the high CBR values indicate strong resistance to deformation under traffic loading, contributing to long-term pavement performance and reduced maintenance needs.

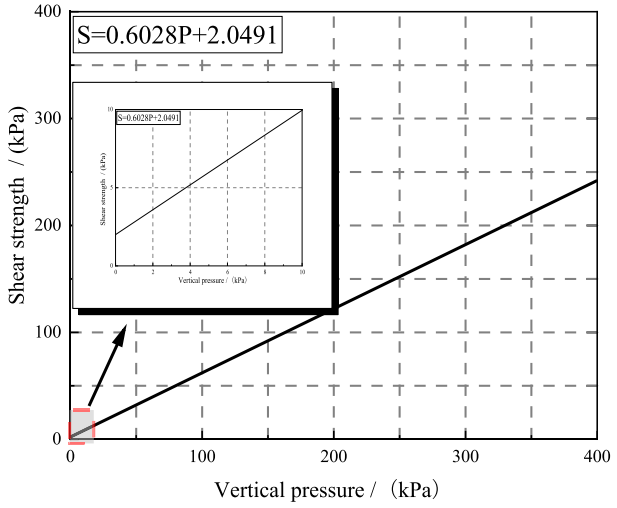

FIGURE 6
Fitting curve of the direct shear test of limestone tailings.

FIGURE 7
Triaxial consolidation drainage shear test device.

3.3 Shear test

3.3.1 Direct shear test

Based on the preliminary test results from the research group, the cohesion and internal friction angle of the control group gravel are 0.1 kPa and 40°, respectively. According to the JTG 3430-2020, direct shear test samples were prepared using limestone tailings material. The test results were calculated using the following Equation 1:

$$S = 10CR/A \tag{1}$$

Where: S is the shear stress (kPa); 10 is a conversion factor; C is the calibration coefficient of the load cell (N/0.01 mm); R is the reading of the load cell (0.01 mm); A is the initial area of the sample (cm^2).

The results of the direct shear tests for the limestone tailings material, along with the fitted shear strength envelope, are shown in Figure 6.

Based on the linear regression of the shear stress *versus* normal stress data, the cohesion (c) and internal friction angle (φ) of the limestone tailings were determined to be 2.05 kPa and 31.08°, respectively. The relatively high internal friction angle is primarily attributed to the physical characteristics of the limestone tailings. Specifically, the particles exhibit rough and angular surfaces, which enhance interparticle friction and mechanical interlocking under shear loading. These surface features significantly contribute to the shear strength by resisting particle rearrangement and slippage, resulting in a higher internal friction angle compared to more rounded or smooth materials. On the other hand, the measured cohesion value is relatively low. This can be explained by the low content of fine particles (particle size <0.005 mm) within the limestone tailings. Fines typically contribute to apparent cohesion in granular soils by filling the voids between larger particles and facilitating interparticle bonding through capillary or electrochemical forces. In the case of limestone tailings, the scarcity of such fine particles limits these cohesive mechanisms, thereby reducing the overall cohesive strength component. These results suggest that the shear strength of limestone tailings is predominantly governed by internal friction rather than cohesion, which is characteristic of coarse granular materials. This behavior should be considered in engineering applications, especially in slope stability, bearing capacity assessments, and compaction control strategies.

3.3.2 Triaxial consolidation drained shear test

The direct shear tests provide the shear strength parameters of the sample, but triaxial consolidation drained shear tests offer more realistic and reliable indicators of shear strength (Sonnekus and Smith, 2022; Gong et al., 2020; Chen et al., 2020). Based on this, both direct shear tests and triaxial consolidation drained shear tests were used to measure the shear strength parameters of limestone tailings in this study. The cylindrical samples used in the triaxial tests were prepared with a height of 80 mm and a diameter of 39.1 mm, following standard geotechnical testing protocols, as shown in Figure 7.

To comprehensively evaluate the shear strength behavior of limestone tailings under different stress conditions, three confining pressures (200 kPa, 400 kPa, and 600 kPa) were selected for the consolidated-drained triaxial shear tests. The test results were calculated using the following Equations 2–4.

$$\varepsilon_1 = \frac{\Delta h_i}{h_0} \tag{2}$$

Where: ε_1 is the axial strain value (%); Δh_i is the height change during the shearing process (mm); h_0 is the initial height of the specimen (mm).

$$A_a = \frac{A_0}{1-\varepsilon_1} \tag{3}$$

Where: A_a is the corrected cross-sectional area of the sample (cm^2); A_0 is the initial area of the specimen (cm^2); ε_1 is the axial strain (mm).

$$\sigma_1 - \sigma_3 = \frac{CR}{A_a} \times 10 \tag{4}$$

Where: σ_1 is the major principal stress (kPa); σ_3 is the minor principal stress (kPa); C is the correction coefficient of the dynamometer (N/0.01 mm); R is the dynamometer readings.

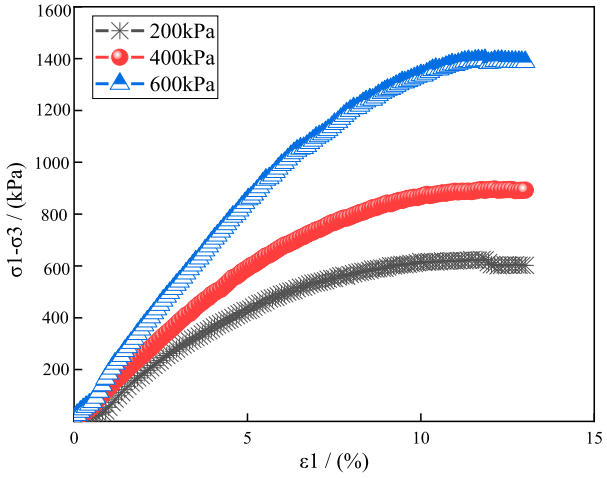

FIGURE 8
Triaxial shear test fitting curves of limestone tailings under different confining pressures.

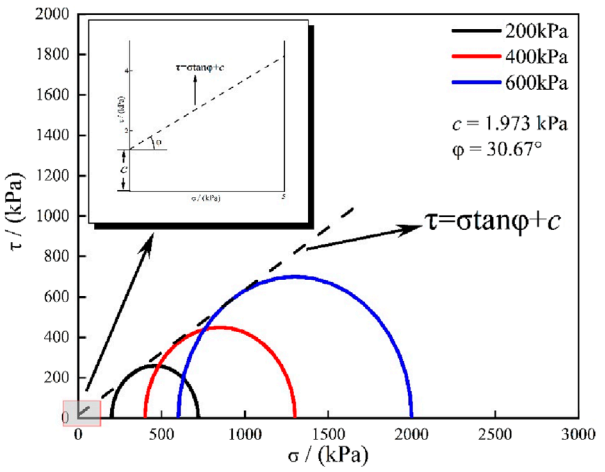

FIGURE 9
Strength envelope of limestone tailings sample.

Figure 8 shows the stress-strain curve of limestone tailings obtained from the triaxial consolidation drained tests. It can be observed that the stress-strain curves under different confining pressures exhibit a strain-hardening behavior, with an approximately linear response during the initial loading stage (ε < 6%). After a strain of about 10%, the curves display pronounced non-elastic deformation. Before yielding, the slope of the curve gradually increases with strain. Furthermore, under the same strain rate, the peak stress varies significantly with confining pressure. As the confining pressure increases, the peak deviatoric stress also rises, indicating enhanced shear strength. This is attributed to the increased pore water expulsion under higher confining pressures, which leads to a denser and more compact sample structure. As a result, internal resistance to deformation is elevated, confirming that greater confining pressure significantly improves the shear strength characteristics of limestone tailings.

The peak value of $\sigma_1 - \sigma_3$ is taken as the failure point. When there is no peak value, the principal stress difference at 15% axial strain is taken as the failure point. Taking the normal stress as abscissa and the shear stress as ordinate, taking $\frac{\sigma_{1f}+\sigma_{3f}}{2}$ as the center and $\frac{\sigma_{1f}-\sigma_{3f}}{2}$ as the radius on the abscissa (f footnote indicates the state of damage), the damage stress diagram is drawn on the $\tau - \sigma$ stress plane diagram, and the envelope of the damage stress circle under different ambient pressures is drawn, as shown in Figure 9. The inclination angle of the line tangent to the three stress circles defines the internal friction angle (φ), while its intercept on the vertical axis corresponds to the cohesion (c). From Figure 9, it can be seen that the cohesion and internal friction angle of limestone tailings from the triaxial shear test are 1.97 kPa and 30.67°, respectively. These values are very similar to those obtained from the direct shear test, as shown in Figure 6. Although the direct shear and triaxial tests produced similar shear strength parameters, their test conditions differ significantly. The direct shear test applies a constant normal stress with simple shear along a predefined plane, and it lacks control over drainage conditions and stress path evolution, which limits its ability to represent *in-situ* stress states. In contrast, the triaxial test better replicates the isotropic or anisotropic stress conditions encountered in subgrade engineering, providing more realistic insights into the material's behavior under embankment loading. Due to these advantages, the strength parameters obtained from the triaxial test were chosen for input in the ABAQUS numerical model, ensuring a closer approximation of field stress conditions and enhancing the accuracy of settlement predictions.

4 Simulation analysis

4.1 Relying on the project introduction

The G207 Xiangyang Xiangzhou to Yicheng Section Reconstruction Project (K55 + 955 to K94 + 309) passes through Nanzhang County, Xiangcheng District, and Yicheng City in Xiangyang. This section is part of the G207 Xiangyang Xiangzhou to Yicheng Reconstruction Project, with the route starting at the boundary between Xiangcheng District and Nanzhang County at chainage K55 + 955 and ending at K94 + 309. The total length of this section is 38.355 km. The route is characterized by the widespread presence of soft soils, primarily consisting of Quaternary alluvial silty clay with a low bearing capacity and poor geotechnical properties, including high water content, high compressibility, and low strength. These soft soils are mainly found around the Jiujiji Interchange and areas such as fishponds and lotus ponds along the route. The total volume of subgrade replacement required is over 1.3 million cubic meters. In line with the national "dual-carbon" strategy and the broader context of sustainable resource utilization, the project proposes the use of limestone tailings as a substitute for natural sand and gravel in subgrade filling.

4.2 Model introduction

In this study, numerical simulation analysis was conducted on the subgrade fill section of silty clay with a clayey silt composition,

TABLE 3 Mechanical parameters of soil material.

Materials	Thickness H/m	Density P/kg•m^{-3}	Elastic modulus E/MPa	Poisson ratio/μ	Cohesion c/kPa	Internal friction angle φ/°
Muddy-silty clay	5.0	1,680	1.9	0.3	10.3	14.7
Gravel	5.0	1900	100	0.3	0.1	40.0
Limestone tailings	5.0	2,350	60	0.3	1.97	30.7

specifically from K66 + 985 to K67 + 005. This section of the route is covered by a hard shell layer, with a maximum thickness ranging from 6.6 to 9 m, and exhibits low bearing capacity along with poor geotechnical characteristics such as high water content, high compressibility, and low strength. The subgrade was treated with limestone tailings, replacing the soft silty clay. The model depth of the subgrade replacement was set to 5 m, with a top width of 25.5 m and a slope of 1:1.5. The cross-sectional length of the subgrade was 84 m, and a 100-m section was selected to establish the model for limestone tailings subgrade fill and analyze the settlement behavior (Feng and Lei, 2022; Yang et al., 2024; Li et al., 2023). The mechanical parameters of the silty clay and limestone tailings are shown in Table 3.

In the simulation calculation of settlement due to subgrade replacement depth, the effect of applied load on settlement was also considered to analyze whether the settlement of the limestone tailings-filled subgrade meets the requirements of the Highway Subgrade Design Specifications (JTG D30-2015) under the most unfavorable conditions. According to the Urban Road Engineering Design Specifications (CJJ37-2012), the applied load is considered as follows: for a primary highway lane, the uniformly distributed load is 10.5 kN/m. Additionally, a 0.67-m-thick asphalt pavement is considered, and the equivalent uniformly distributed load on the upper part of the covered soil is calculated to be 25 kPa.

The ABAQUS software was used to investigate the settlement behavior at the bottom of the subgrade during the filling process of the limestone tailings replacement. The model was established using three-dimensional solid elements, and a total of 20 steps were analyzed. The element type used in the model is C3D8R, the number of elements is 139,774, and the number of nodes is 153,320. The simulation process was structured as follows: Step 1: This step simulates the pre-filling state, where the geostatic equilibrium of the soil model is established after the replacement. Steps 2–19: These steps represent the staged filling of the subgrade. The "dead-and-alive element method" was used, where the subgrade material is initially removed, and then the layers are sequentially activated from bottom to top. For the first 18 layers, the thickness of each layer is 0.3 m, while the final (19th) layer has a thickness of 0.1 m, resulting in a total fill height of 5 m over 19 layers. Step 20: A uniformly distributed load is applied on the upper surface of the soil cover, representing the load of the asphalt pavement and vehicular traffic. The computational model is shown in Figure 10. The mesh size for the subgrade soil elements is 1.0 × 1.0 × 1.0 m, while the mesh size for the limestone tailings filling is 0.1 × 0.1 × 0.1 m.

4.3 Result analysis

The final settlement contour map generated by ABAQUS simulation is shown in Figures 11–13 (settlements at 3 m, 5 m, and 7 m). The stress-strain distribution diagram is also provided, as shown in Figure 14. The elastic-plastic model predicts a maximum settlement of 17.5 cm for the limestone tailings-filled subgrade under 25 kPa load at a 5 m replacement depth. To further explore the time-dependent behavior of the soft soil foundation, two analytical models were introduced for comparison: Mesri-Choi's secondary compression theory and the Sekiguchi-Ohta elasto-viscoplastic model. The Mesri-Choi model estimated long-term settlement due to creep in clay minerals and predicted a settlement of 19.6 cm, highlighting the limitations of standard elastic-plastic models in capturing delayed deformation. The Sekiguchi-Ohta model, which incorporates viscoplastic strain governed by the overstress principle, predicted a settlement of 20.1 cm. This framework considers strain-rate dependency and plastic flow over time, mechanisms not fully represented in ABAQUS's default material library. Although ABAQUS was used for elastic-plastic finite element simulations, the time-dependent deformation was assessed analytically because of the lack of built-in viscoplastic models in the software. Therefore, viscoplastic parameters are not included in Table 3. For future studies, it is recommended to implement viscoplasticity through user-defined subroutines to enable full coupling of time-dependent plasticity within the numerical model. Despite these differences, all models predict settlements well below the allowable limit of 300 mm specified in the JTG D30-2015 standard for soft soil subgrade replacement. This confirms that using limestone tailings as subgrade fill is both structurally feasible and compliant with engineering standards.

5 Settlement monitoring

Settlement monitoring was performed on the subgrade filling section from K66 + 985 to K67 + 005, with the observed settlement curve shown in Figure 15. The monitoring segment K66 + 985–K67 + 005 was selected because pre-construction geotechnical investigations (including boreholes, CPTs, and laboratory index tests) indicated that its stratigraphy, water content, and compressibility are typical of the soft-soil zones along the K55 + 955–K94 + 309 corridor; thus, this reach serves as a representative benchmark for performance validation. Monitoring involved six instrumented stations arranged to capture cross-sectional and longitudinal variability: three on the centerline, two on the

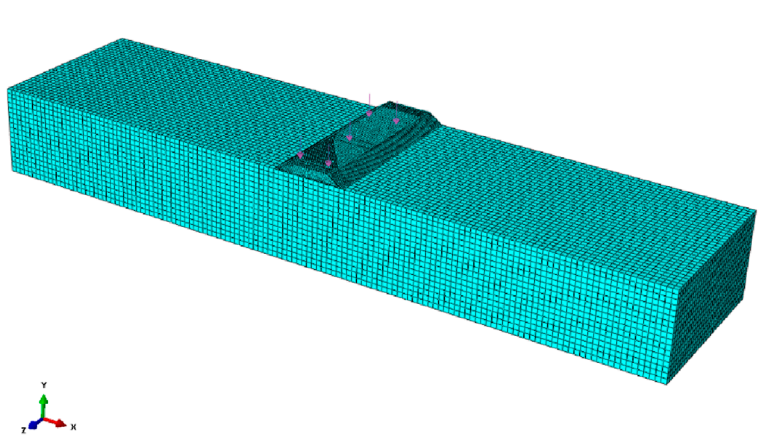

FIGURE 10
Filling subgrade calculation model.

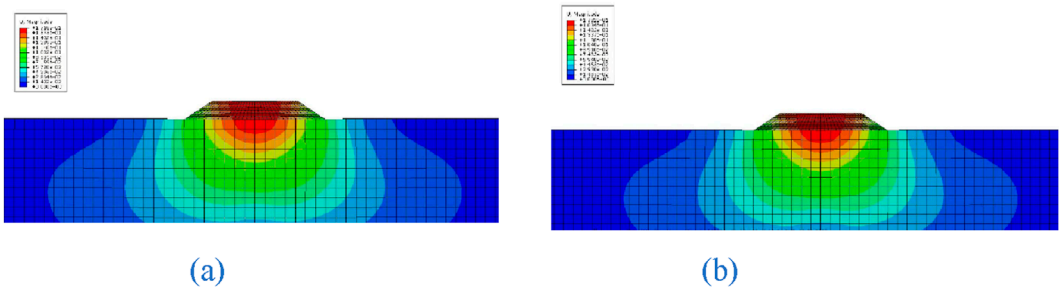

FIGURE 11
Filling subgrade model settlement diagram in 3 m. **(a)** Gravel. **(b)** Limestone tailings.

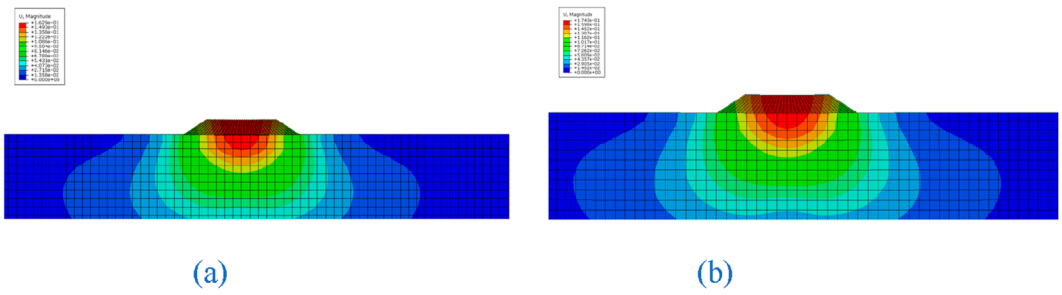

FIGURE 12
Filling subgrade model settlement diagram in 5 m. **(a)** Gravel. **(b)** Limestone tailings.

shoulders, and one at the toe. Each station was equipped with surface settlement plates and settlement pins (at 0.5 m and 1.5 m depths) to monitor near-surface responses. Three of the stations also featured deep benchmarks or inclinometers installed at the fill–foundation interface (around 4.5 m) to track deep settlements and lateral movements. Readings were taken weekly during the first 60 days and monthly thereafter until 200 days. Each data point reflects the average of three repeated measurements; instruments were calibrated before deployment and checked periodically. Settlement stabilized at approximately 16.5 cm after 200 days, slightly lower than the 17.43 cm predicted by the model. This discrepancy is likely due to the actual replacement depth being 4.5 m in the field, which is 0.5 m less than the 5 m depth assumed in the simulation, resulting in simulated settlement being 5.6% higher than the observed settlement. Overall, settlement values for both the subgrade filling and post-construction stages comply with the requirements in JTG D30-2015, confirming the suitability and effectiveness of using limestone tailings for subgrade filling in this case.

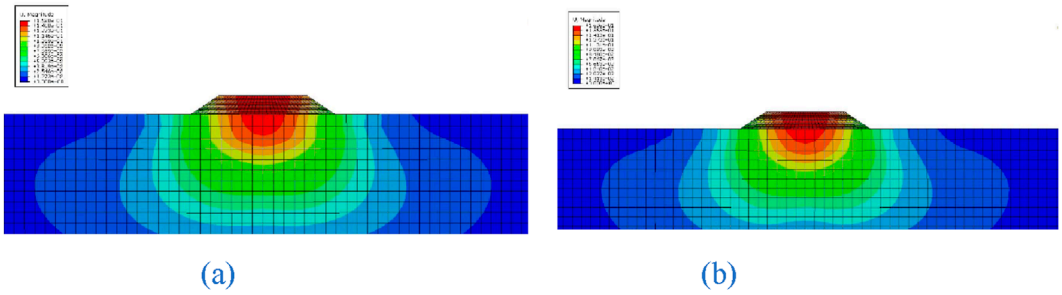

FIGURE 13
Filling subgrade model settlement diagram in 7 m. **(a)** Gravel. **(b)** Limestone tailings.

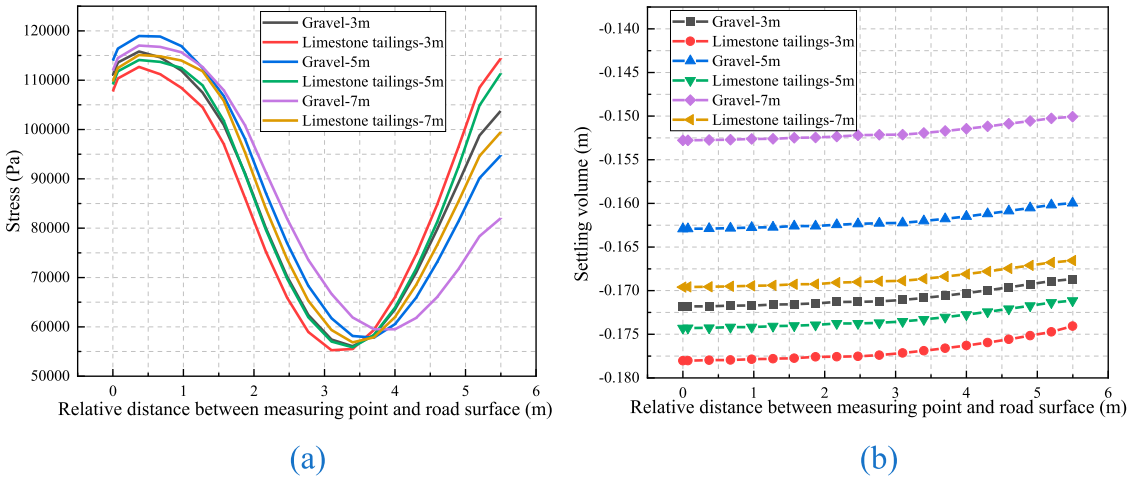

FIGURE 14
Stress and strain distribution. **(a)** Stress distribution. **(b)** Strain distribution.

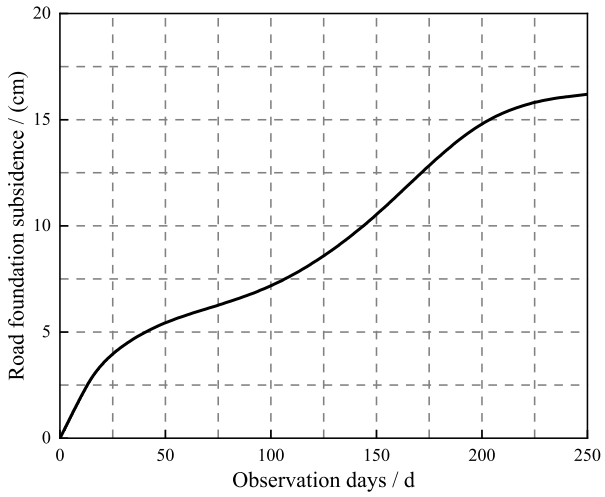

FIGURE 15
Filling subgrade settlement observation curve.

6 Summary and conclusion

This study comprehensively evaluated the feasibility of limestone tailings as sustainable subgrade fillers through experimental characterization, numerical simulation, and field validation. Laboratory tests (XRD, SEM, compaction, CBR, direct/triaxial shear) confirmed optimal gradation, low plasticity, and high bearing capacity (CBR >74%). ABAQUS modeling simulated settlement under extreme conditions (5 m depth, 25 kPa load), predicting 17.43 cm settlement, 5.6% higher than field measurements (16.5 cm) but compliant with JTG D30-2015 standards. The main conclusions and future work are as follows:

1. Limestone tailings exhibit optimal gradation, stable composition, and strong interlocking characteristics, meeting subgrade fill specifications. With optimum moisture content of 4.3% and maximum dry density of 2.283 g/cm^3, their CBR values comply with regulatory standards across varying compaction levels.
2. Shear testing confirms cohesion of 1.97 kPa and internal friction angle of 30.67°, providing precise inputs for

settlement prediction models that enhance computational accuracy.

3. Under extreme conditions (5 m replacement depth and applied load), maximum subgrade settlement remains 0.1743 m, within regulatory compliance limits, validating structural reliability.
4. This study primarily focused on the mechanical properties and short-term performance of limestone tailings mixtures. However, durability under cyclic environmental conditions was not directly evaluated. These degradation mechanisms are particularly relevant in seasonally frozen regions and rainy areas. To comprehensively assess their applicability, future work should include cyclic durability testing, such as wet–dry cycling, freeze–thaw resistance, and sulfate attack tests, combined with microstructural analyses (SEM, MIP, XRD) to reveal deterioration mechanisms.
5. Future research should therefore assess the mechanical and durability performance of composite structures that combine limestone tailings with other stabilizing agents or reinforcement layers. Laboratory model tests, large-scale field trials, and numerical simulations could be integrated to examine how tailings interact with cementitious binders or geosynthetic reinforcements and to establish design guidelines for sustainable composite subgrade applications.

Data availability statement

The original contributions presented in the study are included in the article/supplementary material, further inquiries can be directed to the corresponding author.

Author contributions

CZ: Writing – review and editing, Writing – original draft. WL: Writing – review and editing, Writing – original draft, Visualization, Supervision. CL: Methodology, Data curation, Writing – review and editing, Writing – original draft, Formal Analysis. WZ: Data curation, Writing – original draft. WC: Writing – review and editing. PY: Writing – original draft. XL: Writing – original draft.

Funding

The author(s) declare that financial support was received for the research and/or publication of this article. This study is sponsored by the BUCEA Doctor Graduate Scientific Research Ability Improvement Project (DG2024019), the National Key R&D Program of China (2022YFC3803403), and the Project of Construction and Support for high-level Innovative Teams of Beijing Municipal Institutions (BPHR20220109).

Conflict of interest

Authors CZ, WL, and WC were employed by No.1 Engineering Co., Ltd., CCCC First Highway Engineering.

The remaining authors declare that the research was conducted in the absence of any commercial or financial relationships that could be construed as a potential conflict of interest.

Generative AI statement

The author(s) declare that no Generative AI was used in the creation of this manuscript.

Any alternative text (alt text) provided alongside figures in this article has been generated by Frontiers with the support of artificial intelligence and reasonable efforts have been made to ensure accuracy, including review by the authors wherever possible. If you identify any issues, please contact us.

Publisher's note

References

Adewuyi, S. O., Anani, A., and Luxbacher, K. (2024). Advancing sustainable and circular mining through solid-liquid recovery of mine tailings. *PROCESS Saf. Environ. Prot.* 189, 31–46. doi:10.1016/j.psep.2024.06.086

Chen, Q. Z., Liu, Y. M., and Pu, S. Y. (2020). Strength characteristics of nonpenetrating joint rock mass under different shear conditions. *Adv. Civ. Eng.* 2020, 3579725. doi:10.1155/2020/3579725

Chu, C. F., Zhan, M. H., Feng, Q., Deng, Y. F., Li, D., Zha, F. S., et al. (2023). Expansive soil modified by iron tailing sand and calcium carbide slag as subgrade material. *Environ. Dev. Sustain.* 25 (9), 10393–10410. doi:10.1007/s10668-022-02498-x

de Matos, P. R., Doerner, G., Nazário, S. da S., Andrade Neto, J. da S., Longhi, M., Folgueras, M., et al. (2025). Limestone calcined clay cements (Lc^3) produced with iron ore tailings and ceramic waste: hydration, mechanical performance and rheology. *Constr. Build. Mater.* 458. doi:10.1016/j.conbuildmat.2024.139604

Feng, S. X., and Lei, H. Y. (2022). A settlement prediction model considering tidal loading and traffic loading of soft soil subgrade. *Comput. GEOTECHNICS* 144, 104639. doi:10.1016/j.compgeo.2022.104639

Gallage, C., Jayakody, S., Abeykoon, T., Biyanvilage, D., and Rajapakse, J. (2024). A laboratory-based test procedure for the investigation of slaking-induced changes in geotechnical properties of tailing dam embankment materials. *HELIYON* 10 (4). doi:10.1016/j.heliyon.2024.e26489

Gao, H., An, B., Dai, Y., Fan, K., Ding, J., and Liu, H. (2025). Utilizing of graphite tailings as fine aggregates in asphalt mixture: road performance and economic environment assessments. *CASE Stud. Constr. Mater.* 22. doi:10.1016/j.cscm.2025.e04807

Gong, F. Q., Luo, S., Lin, G., and Li, X. B. (2020). Evaluation of shear strength parameters of rocks by preset angle shear, direct shear and triaxial compression tests. *ROCK Mech. ROCK Eng.* 53 (5), 2505–2519. doi:10.1007/s00603-020-02050-1

Gou, M. F., Zhou, L. F., and Then, N. W. Y. (2019). Utilization of tailings in cement and concrete: a review. *Sci. Eng. Compos. Mater.* 26 (1), 449–464. doi:10.1515/secm-2019-0029

Gupta, S., Kumar, S., Pradeep, N. M., and Nishant, M. (2025). Performance analysis of soil-geopolymer deep mix column in soft soil under static and cyclic loading. *SOIL Dyn. Earthq. Eng.* 194, 109368. doi:10.1016/j.soildyn.2025.109368

Kong, Y. H., Zhang, X., Zhang, L., Xu, J., Ji, W., Pan, L., et al. (2024). Investigation on utilization and microstructure of fine iron tailing slag in road subbase construction. *Constr. Build. Mater.* 447, 138019. doi:10.1016/j.conbuildmat.2024.138019

Li, H. B., Cui, C. Y., Sheng, Y. P., Zhang, M., Feng, Z., Li, L., et al. (2023). Application of composite steel slag as subgrade filler: performance evaluation and enhancement. *Constr. Build. Mater.* 370, 130448. doi:10.1016/j.conbuildmat.2023.130448

Li, S., Zhang, Z., Si, C., Shi, X., Cui, Y., Bao, B., et al. (2025). Evaluation of the rheological properties of asphalt mastic incorporating iron tailings filler as an alternative to limestone filler. *J. Clean. Prod.* 486. doi:10.1016/j.jclepro.2024.144444

Liang, Q. P., Zhang, S. T., Zhang, N., Ge, Z., Lv, L., Ling, Y., et al. (2024). Properties of lightweight foamed concrete containing gold tailings as subgrade filler. *Struct. Concr.*, suco.202300580. doi:10.1002/suco.202300580

Liao, J., Xu, S. Y., Zhang, C. C., Bai, G. J., and Li, T. Y. (2025). Experimental study on the consolidation characteristics of soilbags-reinforced soft soil foundation with surcharge preloading. *CASE Stud. Constr. Mater.* 22, e04746. doi:10.1016/j.cscm.2025.e04746

Liu, Z., Gao, Y., Liao, J., and Zhou, C. Y. (2022). Stochastic medium model for the settlement calculation of prefabricated vertical drains of soft soil foundations in the coastal area of south China. *J. Mar. Sci. Eng.* 10 (7), 867. doi:10.3390/jmse10070867

Liu, H. B., Deng, S. W., Zhao, L. N., Yang, L., Qi, J. H., and Jiang, Y. J. (2024a). Turning waste into treasure: utilizing environment-pollutant graphite tailings as photocatalyst for photocatalytic building materials. *CASE Stud. Constr. Mater.* 21, e03859. doi:10.1016/j.cscm.2024.e03859

Liu, H., An, B., Liu, L., Song, J., Ding, J., and Gao, H. (2024b). Recycling of graphite tailings: effect of graphite tailings on property asphalt mortar and environmental impact evaluation. *Constr. Build. Mater.* 452. doi:10.1016/j.conbuildmat.2024.138859

Maruthupandian, S., Chaliasou, A., and Kanellopoulos, A. (2021). Recycling mine tailings as precursors for cementitious binders – methods, challenges and future outlook. *Constr. Build. Mater.* 312. doi:10.1016/j.conbuildmat.2021.125333

Ou, X. D., Chen, S. J., Jiang, J., Qin, J. X., and Zhang, L. (2022). Reuse of red mud and bauxite tailings mud as subgrade materials from the perspective of mechanical properties. *MATERIALS* 15 (3), 1123. doi:10.3390/ma15031123

Panchal, S., Deb, D., and Sreenivas, T. (2018). Mill tailings based composites as paste backfill in mines of U-bearing dolomitic limestone ore. *J. ROCK Mech. GEOTECHNICAL Eng.* 10 (2), 310–322. doi:10.1016/j.jrmge.2017.08.004

Sa, T. S. W., Oda, S., Balthar, V., and Toledo, R. D. (2022). Use of iron ore tailings and sediments on pavement structure. *Constr. Build. Mater.* 342, 128072. doi:10.1016/j.conbuildmat.2022.128072

Shanmugasundaram, V., and Shanmugam, B. (2023). Application of cement treated magnesite mine tailings as subgrade. *Constr. Build. Mater.* 365, 130064. doi:10.1016/j.conbuildmat.2022.130064

Singh, S., Kumar, A., and Sitharam, T. G. (2024). Experimental study on strength, durability, hydraulic and Toxicity characteristics of soil treated with mine tailings based Geopolymers for sustainable road subgrade application. *Constr. Build. Mater.* 414. doi:10.1016/j.conbuildmat.2024.134894

Song, Q., Su, J. H., Nie, J., Li, H., Hu, Y., Chen, Y., et al. (2021). The Occurrence of Mgo and its influence on properties of clinker and cement: a review. *Constr. Build. Mater.* 293, 123494. doi:10.1016/j.conbuildmat.2021.123494

Sonnekus, M. C. H., and Smith, J. V. (2022). Comparing shear strength dispersion characteristics of the triaxial and direct shear methods for undisturbed dense sand. *KSCE J. Civ. Eng.* 26 (4), 1560–1568. doi:10.1007/s12205-022-0040-6

Su, C. X., Rana, N. M., Zhang, S., and Wang, B. J. (2024). Environmental pollution and human health risk due to tailings storage facilities in China. *Sci. TOTAL Environ.* 928, 172437. doi:10.1016/j.scitotenv.2024.172437

Sun, Yu, Yu, R., Wang, S., Zhou, Y., Zeng, M., Hu, F., et al. (2021). Development of a novel eco-efficient Lc2 conceptual cement based ultra-high performance concrete (uhpc) incorporating limestone powder and calcined clay tailings: design and performances. *J. Clean. Prod.* 315. doi:10.1016/j.jclepro.2021.128236

Wang Y. S, Y. S., Li, Z. F., Jin, Q., Zhang, M., and Zhou, Z. H. (2022). High-efficiency utilization of limestone tailings: used as cementitious materials and fine aggregate to prepare karst structure filling material. *Constr. Build. Mater.* 316, 125841. doi:10.1016/j.conbuildmat.2021.125841

Wang Z. Q, Z. Q., Chu, H. C., Wang, J. X., Feng, E. J., Zhang, Y., and Lyu, X. J. (2022). Mechanical activation of siliceous tailings and its application as cement admixtures. *Miner. Eng.* 177, 107366. doi:10.1016/j.mineng.2021.107366

Wu, C., Li, J., Lu, Y., and Zhu, D. (2024). The influence of industrial solid waste in conjunction with lepidolite tailings on the mechanical properties and microstructure of cemented backfill materials. *Constr. Build. Mater.* 419. doi:10.1016/j.conbuildmat.2024.135422

Xiong, F., Wang, X. B., Yang, F., Yang, J. Q., Hu, L., and Li, R. (2022). Analytical and numerical study on the stability of highway subgrade with embedded loading berm in soft soil area. *Appl. SCIENCES-BASEL* 12 (23), 12440. doi:10.3390/app122312440

Xu, J. B., Wang, Y. Z., Yan, C. G., Zhang, L., Yin, L., Zhang, S., et al. (2019). Lifecycle health monitoring and assessment system of soft soil subgrade for expressways in China. *J. Clean. Prod.* 235, 138–145. doi:10.1016/j.jclepro.2019.06.256

Xu, M., Hu, L., Qian, Z., Dong, Z., and Mo, L. (2025). Effects of fluorite tailings content on formation, properties and fluorine doping preferences of high-silica clinker: experimental study and industrial verification. *J. Build. Eng.* 106. doi:10.1016/j.jobe.2025.112612

Yang, C. W., Xu, X. Q., Yue, M., Luo, J., Su, K., Ma, H., et al. (2024). Abaqus-based research on the parameters of highway subgrade vibratory compaction and vibration wave propagation laws. *Sci. Rep.* 14 (1), 29635. doi:10.1038/s41598-024-80357-7

Yin, P., Wang, J., He, W., Wang, S., Li, X., and Jia, Z. (2024). Machine learning-based study on the mechanical properties and embankment settlement prediction model of nickel–iron slag modified soil. *Constr. Build. Mater.* 431. doi:10.1016/j.conbuildmat.2024.136468

Yu, Y. H., and Du, C. M. (2023). Leaching of phosphorus from phosphate tailings and extraction of calcium phosphates: toward comprehensive utilization of tailing resources. *J. Environ. Manag.* 347, 119159. doi:10.1016/j.jenvman.2023.119159

Zhang, S. X., Liu, F. Y., Ying, M. J., and Zeng, W. X. (2024). Test and prediction for the shear behavior of the sand-irregular concrete interface under constant and dynamic normal loading. *SOIL Dyn. Earthq. Eng.* 180, 108620. doi:10.1016/j.soildyn.2024.108620

Zhang M, M., Lv, H., Jiang, Q., Wu, Y., Yang, Y., and Dai, H. (2025). Study on flexural behavior of laminated slabs constructed with composite limestone powder-tailings mixed sand concrete. *STRUCTURES* 77. doi:10.1016/j.istruc.2025.109169

Zhang Z. Q, Z. Q., Shao, H. R., Yu, Q. J., and Yin, S. H. (2025). Hydration performance and carbon reduction potential of limestone calcined clay cement (Lc3) derived from shield spoil tailings: from waste to sustainable binder. *Constr. Build. Mater.* 485, 141854. doi:10.1016/j.conbuildmat.2025.141854

Zhao, X. Q., Yang, T. F., Zong, Z. L., Liang, T., Shen, Z. Y., Li, J. W., et al. (2024). Study on mechanical properties of phosphate tailings modified clay as subgrade filler. *Geomech. Eng.* 36 (6), 619–629. doi:10.12989/gae.2024.36.6.619

Zhou, L. F., Gou, M. F., and Guan, X. M. (2021). Hydration kinetics of cement-calcined activated bauxite tailings composite binder. *Constr. Build. Mater.* 301, 124296. doi:10.1016/j.conbuildmat.2021.124296

Zhu, J. –feng, Wang, Z. –qing, Tao, Y. –li, Ju, L. –ying, and Yang, H. (2024). Macro–micro investigation on stabilization sludge as subgrade filler by the ternary blending of steel slag and fly ash and calcium carbide residue. *J. Clean. Prod.* 447, 141496. doi:10.1016/j.jclepro.2024.141496